Available online at www.sciencedirect.com
SCIENCE DIRECT®
Thin Solid Films 453–454 (2004) 195–202
thin solid films
www.elsevier.com/locate/tsf

Structural, mechanical and tribological investigations of pulsed laser deposited titanium nitride coatings

J.M. Lackner[a,b,c,*], W. Waldhauser[b], R. Berghauser[b], R. Ebner[a,b], B. Major[d], T. Schöberl[e]

[a]Materials Center Leoben, Franz-Josef-Strasse 13, A-8700 Leoben, Austria
[b]Laser Center Leoben, JOANNEUM RESEARCH Forschungsgesellschaft mbH, Leoben, Leobner Strasse 94, A-8712 Niklasdorf, Austria
[c]Institute of Physical Metallurgy and Materials Testing, University of Leoben, Franz-Josef-Strasse 18, A-8700 Leoben, Austria
[d]Institute of Metallurgy and Materials Science, Polish Academy of Sciences, ul. Reymonta 25, 30-059 Cracow, Poland
[e]Erich Schmid Institute, Austrian Academy of Sciences, Jahnstrasse 12, A-8700 Leoben, Austria

Abstract

The high hardness and the low-wear rates characterize the outstanding tribological behaviour of titanium nitride (TiN) making it to the most widespread material for hard coatings, which were deposited industrially in recent years by employing various deposition methods. For coating of heat sensitive materials and machine parts at low temperatures down to room temperature, only a few deposition techniques can be applied. One of these is the pulsed laser deposition (PLD) method. In this work a multi-spot PLD system with four Nd:YAG laser beams (1064-nm wavelength) was applied to vaporize titanium targets in low-pressure N_2 atmospheres at room temperature. For the deposition of the TiN coatings, high speed tool steel (AISI M2) and corrosion resistant steel (AISI 630 HT) substrates were used. To investigate the differences of film growth in dependency of the target–substrate arrangement, the substrate surfaces were situated parallel (on-axis) and rectangular (off-axis) to the target. The coatings were examined by light-microscopy, scanning electron microscopy, X-ray diffraction, nanoindentation and pin-on-disc tests against ball-bearing steel (DIN 100Cr6/AISI 52100) and alumina (Al_2O_3) counterparts. The results indicate a high influence of the target–substrate arrangement on the textures, residual stresses and hardnesses of the TiN coatings. In spite of these differences all coatings on both on-axis and off-axis placed substrates possess excellent adhesion and high-wear resistance.

Keywords: Pulsed laser deposition; Laser ablation; Titanium nitride; Low-wear

1. Introduction

Titanium nitride (TiN) is a well-known coating material for improving the tribological performance of tools and machine parts in industrial applications. A significant increase of tool lifetime can be achieved by using TiN coatings commonly formed by various chemical vapour deposition (CVD) and physical vapour deposition (PVD) techniques [1]. For the deposition of TiN coatings, these methods require elevated substrate temperatures higher than 200–500 °C to achieve a good adhesion on the substrates and a high hardness. These high-substrate temperatures inhibit the use of TiN coatings in many applications where the substrates (e.g. pre-stressed tools) or substrate materials (e.g. plastics, compounds) cannot withstand such high temperatures. Thus, there is a high demand for developing low-temperature deposition processes for hard coating materials like TiN, such as the pulsed laser deposition (PLD).

In the PLD technique a pulsed laser beam is focussed onto a target in order to evaporate its surface layers under vacuum or low pressure process gas conditions [2]. The vaporized material consisting of atoms, ions and atomic clusters is then deposited onto the substrate. The outstanding advantage of this technique is the possibility to deposit coatings of very high chemical purity and adhesion to various substrate materials at room temperature. Furthermore, high rate film growth on surface areas situated perpendicular to the targets surface is also possible by using a low-pressure process gas. The application of reactive process gases leads to the opportunity of varying the film stoichiometry in a wide range.

*Corresponding author. Tel.: +43-3842-81260-2305; fax: +43-3842-81260-2310.
E-mail address: juergen.lackner@joanneum.at (J.M. Lackner).

0040-6090/04/$ - see front matter © 2003 Elsevier B.V. All rights reserved.
doi:10.1016/j.tsf.2003.11.106

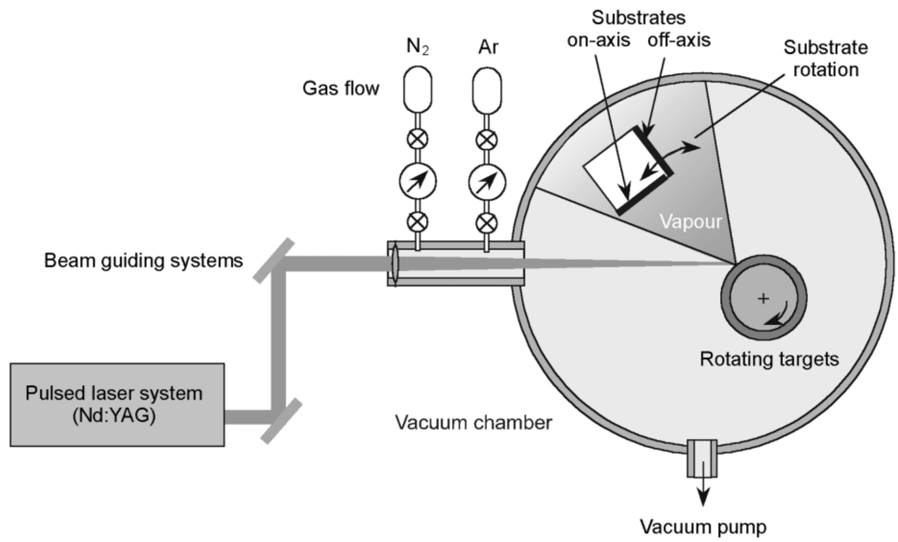

Fig. 1. Schematic view of the PLD system used for TiN film deposition.

The application of the PLD process for the deposition of TiN coatings was shown by several authors in the last years [3–8]. The aim of these published works was the deposition of TiN coatings for microelectronic, decorative and optical purposes because of their high-thermal stability and low-electrical resistance. However, the friction and wear behaviour as well as the influence of the deposition arrangement on the properties of PLD TiN have not been reported in literature so far. Furthermore, the shortcoming of all these works are very small-coated areas, which are much too small for industrial coating processes. Thus, closing this gap and showing the outstanding capability of PLD for deposition of TiN coatings for tribological purposes in industrial applications on large area substrates is the goal of the present study.

2. Experimental details

2.1. Film deposition

High-purity titanium targets were used for the ablation experiments using a pulsed Nd:YAG laser system, which provides four beams of 1064 nm wavelength, 0.6 J pulse energy and 10 ns pulse duration at a repetition rate of 50 Hz [9]. In this multi-spot evaporation system the targets are rotated during the laser irradiation in order to avoid the formation of deep craters. The emitted species were deposited at room temperature ($\approx$25 °C) onto steel substrates mounted parallel (on-axis geometry) as well as normal (off-axis geometry) to the target surface, see Fig. 1. Prior deposition the substrates—ferritic corrosion resistant steel AISI 630 HT and high speed steel AISI M2 with a hardness of 64 HRC—were mirror-polished and cleaned ultrasonically in pure acetone and ethanol. To provide homogenous film thicknesses over the whole coated surfaces, the substrates were moved with a relative speed of 5.4 cm s^{-1} through the plasma plumes during deposition. The reaction chamber was evacuated before starting deposition to pressures below 2×10^{-3} Pa using a pumping unit consisting of a rotary vane pump and a turbomolecular pump. During deposition, the flows of the process gases (Ar, N_2) were adjusted by means of electronic mass flow controllers to a gas flow ratio $N_2/Ar=1/2$.

2.2. Film characterization

The surface quality and structure of the coatings were inspected with light and scanning electron microscopy (SEM; Cambridge Instruments Stereoscan 360). Chemical analyses were performed with wavelength dispersive spectroscopy (WDS).

The phase composition of the TiN coatings were analysed by a X-ray diffractometer (Bruker AXS D8 Discover) using grazing incidence (0.5°, 1.0°, 2.0°) of the primary beam (Cu Kα radiation). The texture and stress analyses were performed using a Philips PW 1710 XRD X-ray diffractometer and Co Kα radiation. For the pole figure measurements, a step size of 2.5° for the polar and azimuthal angle was applied. The X-ray $\sin^2\Psi$ method was used to measure the residual stresses of the first order on the basis of diffraction line shifting.

The hardnesses and elastic moduli of the coatings were measured by nanoindentation with Berkovich indenters. The applied maximum loads were 11 mN, the loading rates 20 nm s^{-1} for all measurements. Apart

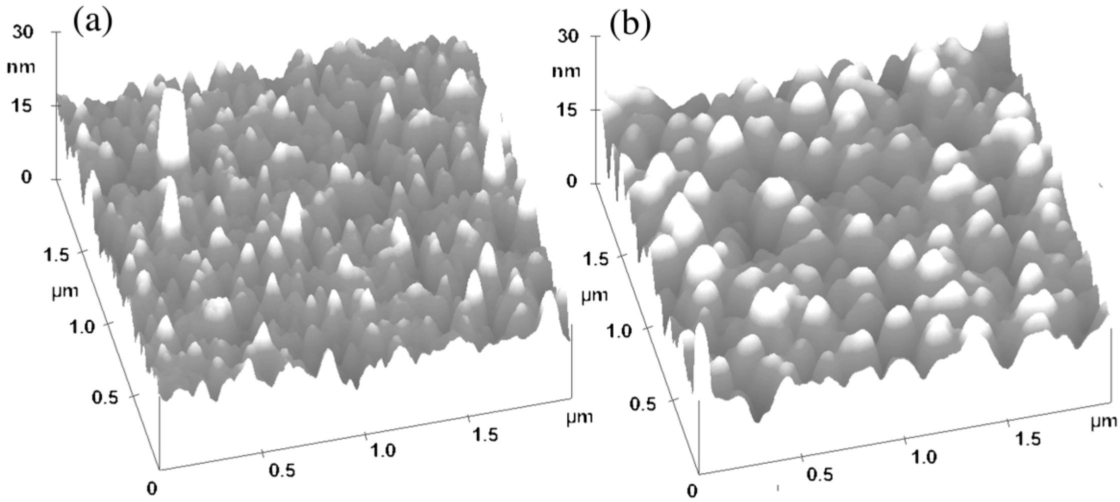

Fig. 2. AFM micrographs of a (a) on-axis and (b) off-axis grown TiN coating.

from mechanical investigations this apparatus was also used for atomic force microscopy (AFM).

The dry sliding friction of the TiN coatings at room temperature (25 °C) was evaluated using a CSEM Instruments high-temperature pin-on-disc tribometer with 6 mm AISI 52100 (DIN 100Cr6) ball-bearing steel balls and Al_2O_3 balls as counterparts. All experiments were carried out on the as-deposited, ultrasonically cleaned surfaces. The applied load was 10 N at a sliding speed of 0.1 $m\,s^{-1}$. The relative humidity during the measurements was adjusted at approximately 60%. The wear tracks were inspected by optical profilometry (Veeco NT-1000) to determine wear mechanisms and wear rates.

3. Results and discussion

3.1. Structure, texture and composition of the films

After deposition of the TiN coatings, light microscopy inspections of the surfaces revealed excellent film quality with only small amounts of defects. The round-shaped defects found with a maximum diameter of 1 μm originate in the ablation process of the target surface. Apart from ions, atoms and clusters also molten particulates (droplets) are ejected during laser–target interaction [2]. For the coatings deposited in the on-axis geometry, slightly higher densities of droplets (11 400 mm^{-2}) were found than for off-axis grown films (10 900 mm^{-2}).

For characterizing the surfaces on the nanometer scale, AFM investigations were performed on the on-axis and off-axis grown coatings (Fig. 2). In both cases nanoclustered surfaces were found, the approximate double size of the nanoclusters of the off-axis coating (∼150 nm) refers to significant lower energies of the deposited species compared to the on-axis grown coatings. This influence of the lower particle energy on the film growth mechanism is well known for PVD coatings [10] and is caused in our case by the overwhelming necessity of scattering of the ablated species with process gas atoms for reaching the off-axis situated substrate surface. The loss of particle energy during scattering leads to a lower activation of surface diffusion processes [11] and a decreased film nucleation rate by the reduced amount of incorporated point defects in the film [12] resulting in the coarser nanoclusters found for the off-axis coating.

The thicknesses and structures of the TiN coatings deposited were detected on fracture cross-sections by SEM. Both, on-axis and off-axis grown, coatings (Fig. 3) possess a micro-columnare microstructure, compareable to the Zone-T structure of Thornton's structure zone model [10]. According to the AFM investigations, coarser micro-columns can be observed for the off-axis grown films, indicating film growth by particles of lower energy. The necessity of scattering with other atoms in the process gas for reaching the off-axis mounted substrates influences the deposition rate of the coatings too. Thus, the deposition yield values were found significantly smaller for the off-axis coatings leading to film thicknesses of 0.9 μm compared to 1.6 μm of the on-axis grown coatings.

Further influences of the different deposition conditions were found in the phase analysis performed by depth-sensitive XRD in grazing incidence arrangement. Typical XRD spectra at incidence angles of the primary X-ray beam of 0.5°, 1.0° and 2.0° are shown in Fig. 4 for on-axis and off-axis grown TiN coatings. In these spectra the labeled peaks correspond to the coating

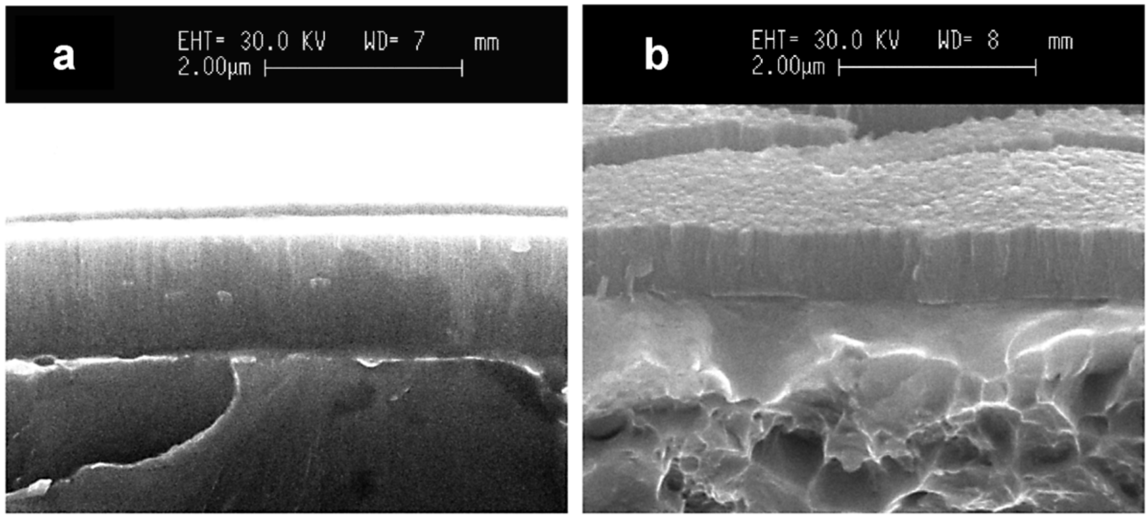

Fig. 3. SEM micrographs of fracture sections of a (a) on-axis and (b) off-axis grown TiN coatings.

(TiN) and the ferritic steel substrate (Fe) reflections. For both coatings, the XRD spectra show the face-centered cubic structure of stoichiometric TiN with the strongest reflections in the (1 1 1) orientation. In addition, (2 0 0) TiN reflexions and small peaks of (2 2 0)- and (3 1 1)-orientated crystals parallel to the surface are present in the on-axis coating. The strong (1 1 1) reflections refer to high stresses in the coatings, because (1 1 1) lattice planes possess in TiN the lowest lattice strain energies compared to (2 0 0) or (2 2 0) planes [14] due to the anisotropy of its elastic constants [13]. Thus, this structure is thermodynamically favourited due to residual stress minimization in the coatings deposited at low temperatures and high ion bombardment [15]. The high energetic ion bombardment (Ti, Ar, N ions) results in a deep penetration of the ions into the grown coating. Inelastic collision cascades of these species with film atoms leading to a decrease of their energy as well as to the incorporation of the penetrated species result in high distortion of the TiN crystal lattice. Both effects cause high lattice distortion and stresses, leading to the development of (1 1 1) structures [16,17]. The (2 0 0) reflection, which is found in addition to the (1 1 1) TiN peak in the on-axis grown coatings, indicates generally high kinetic energy of the deposited species during the growth of the coatings too. The high energy enables in these coatings deposited at room temperature a healing of surface-near growth defects by surface diffusion. Thus, the distortion of the lattice is small, leading to the preferred growth of the (2 0 0) planes parallel to the surface due to their low surface energy [18–20]. Comparing the (2 0 0) peak intensity in dependence of the incidence angle and the TiN (1 1 1) reflection, a decrease of the intensity ratio of TiN (2 0 0)/TiN (1 1 1) at higher incidence angles (deeper penetration of the primary X-ray beam) can be observed which is due to interface-induced growth stresses.

Owing to the different situated substrates, the ablated species strike the substrate surface under different angles revealing in the texture analyses of the TiN coatings (Fig. 5): For the on-axis grown film (Fig. 5a) a typical film fiber texture with the dominant component {1 1 0} ⟨0 1 1⟩ was found. In contrast, the off-axis film is not fiber textured, the dominant texture component is {1 1 2} ⟨2 2 3⟩ (Fig. 5b). Furthermore, a tilt is found in the main crystallite orientation of the coating. According to the texture analysis of plasma immersion ion implanted TiN films [21] this tilt can be attributed to the slope in the impinging angle of the deposited species. Also to exclude influences of the substrate material, the

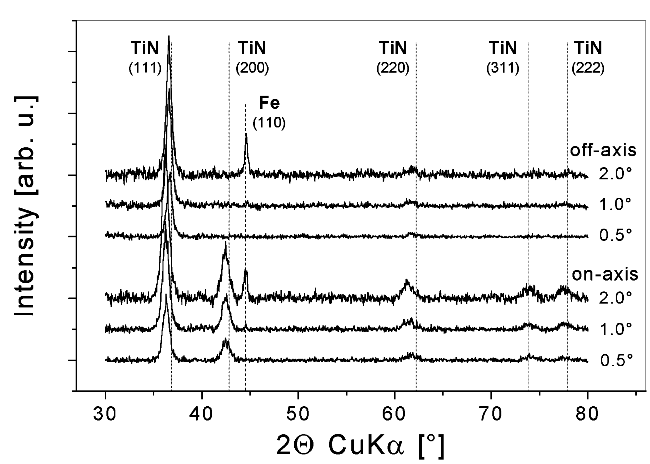

Fig. 4. XRD spectra of on-axis and off-axis grown TiN coatings analysed in grazing incidence alignment with incidence angles of the primary X-ray beam of 0.5°, 1.0° and 2.0° (Fe: ferritic steel substrate AISI 630 HT, TiN: coating).

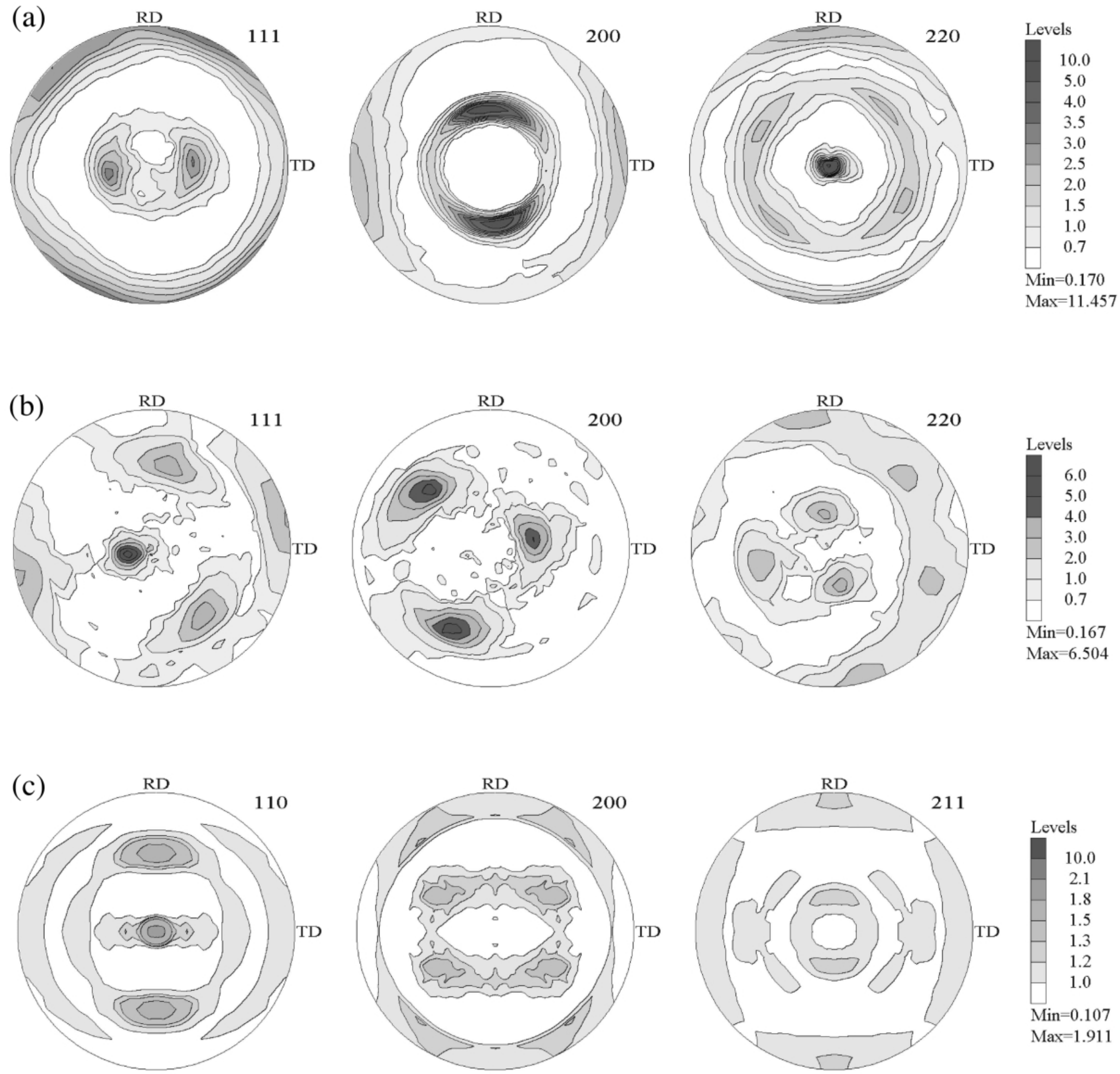

Fig. 5. Pol figures of (a) the on-axis, (b) the off-axis grown TiN coating and (c) the uncoated substrate (AISI 630 HT ferritic steel).

textures of the substrate of both coatings were investigated revealing similar pol figures (rolling texture {1 1 0} ⟨1 1 2⟩) for both types of coatings (Fig. 5c).

In spite of the completely different deposition conditions the chemical compositions of both coating types are similar. WDS investigations showed nearly stoichiometric compositions (TiN) with Ti/N atom ratios of typically 1 ± 0.05 for all coatings investigated.

3.2. Mechanical properties of the films

A further influence of the lower energy of the deposited species was found in the XRD residual stress measurements revealing compressive stresses σ_{11} of approximately -2800 ± 255 and -8100 ± 850 MPa for the off-axis and on-axis grown coatings, respectively (Table 1). These high compressive stresses in the PLD TiN coatings are in accordance to previous examinations [22] and are caused by the incorporation of high energetic atoms and ions in the grown coating. Due to the very dense structure (Fig. 3) of the coatings a relaxation of the stresses by decreasing intercolumnar pores is not possible [23]. Furthermore, bulk diffusion cannot be activated at the low substrate temperatures, which prevents a stress relaxation too.

The high lattice distortion increases the ultra-micro hardnesses and the reduced elastic moduli of the coatings, investigated using depth-sensing nanoindentation tests (Table 1). These mechanical properties of on-axis and off-axis grown PLD TiN coatings are high compared to films deposited by other PVD or CVD techniques [24].

Inspite of these high residual stresses and high hardnesses the adhesion of the TiN coatings to the substrate materials is excellent. Adhesion tests of both types of TiN coatings applying the Rockwell indentation method [25] were recently reported in detail [26], indicating the best adhesion (adhesive strength class HF 1 on the six-part scale from 1 to 6) characterized by only a few cracks and a missing of delaminated coating areas around the indentations.

3.3. Tribological properties of the films

The friction and wear behaviour of the films were investigated by pin-on-disc tests against uncoated ball-bearing steel (AISI 52100, DIN 100Cr6) and alumina (Al_2O_3) counterparts at room temperature. Two stages of the development of friction were found in dependence of the sliding distance (Fig. 6a):

(1) The initial friction coefficients in the run-in period (~10 m of sliding) are influenced by the initial roughness of the ball and disc surfaces and the chemical reactivity between these two surfaces in contact. The latter effect can be clearly observed in the comparison of the initial friction coefficients of the 100Cr6 and the Al_2O_3 counterparts due to the nearly equal surface roughnesses (R_a=4–5 nm) of all sliding surfaces. The highest initial friction coefficients were found for sliding against 100Cr6 steel ball counterparts because of the immediate growth of an iron transfer-layer on the TiN surface. This layer is visible in SEM investigations of the wear tracks after 5–10 contacts to the 100Cr6 counterpart. The lower initial friction coefficients of the TiN/Al_2O_3 couples might reveal the lower adhesive forces between the two surfaces [1].

(2) The increase of friction during the run-in stage up to average values of approximately 0.8, reached after approximately 10 m of sliding, is caused by different mechanisms: In case of the TiN/100Cr6 couple, sliding occurs on the transfer layer (Fig. 7a) consisting of iron, titanium, nitrogen and oxygen, found in EDS investigations. This result represents the typical friction coefficient for a steel/steel couple. In contrast, highly abrasive wear debris was found in the TiN/Al_2O_3 sliding couples leading to the high friction coefficients and abrasive grinding wear scares on the TiN coated disc (Fig. 7b).

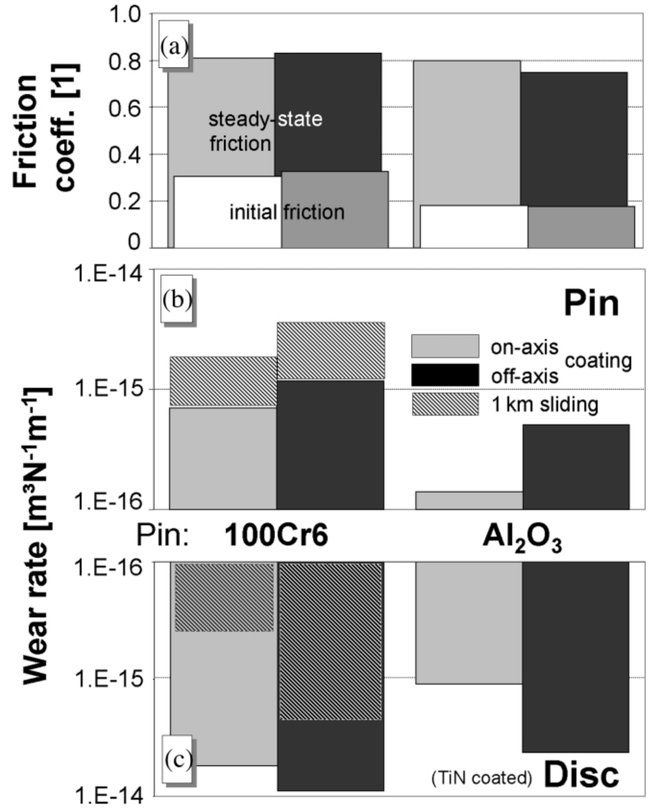

Fig. 6. (a) Initial (bright columns) and steady-state (dark columns) friction coefficients for the TiN/100Cr6 and TiN/Al_2O_3 disc/pin couples. (b) Pin and (c) disc wear rates for on-axis and off-axis grown TiN coatings sliding against 100Cr6 balls and alumina balls (test parameters: sliding distance: 90 m, friction force: 10 N, sliding speed: 0.1 m s^{-1}, temperature: 25 °C, relative humidity: 60%). The striped areas represent the wear rates of the TiN/100Cr6 couple after 1000 m sliding.

The wear rates (Fig. 6b and c) were calculated using the lost volume of the pin and the disc during the pin-on-disc test. For all different sliding couples very low wear rates have been found compared to other PVD/CVD TiN coatings in Ref. [1]. In general, the off-axis grown coatings suffered slightly higher wear than the on-axis films, which could be a reason of the differences in the mechanical properties (lower compressive residual stresses and lower hardness of the off-axis grown films)

Table 1
Lattice stresses, reduced elastic moduli and hardnesses of the substrate, the on-axis and the off-axis grown PLD TiN coatings

	Lattice stress σ_{11} (MPa)	Reduced elastic modulus E (GPa)	Hardness H
Substrate	AISI 30 HT	AISI M2	AISI M2
Substrate	Radial: 260 Transverse: 150	202±4	64 HRC
TiN film (on-axis grown)	−8100±850	311±8	26.5±1.0 GPa
TiN film (off-axis grown)	−2800±255	248±7	16.9±0.8 GPa

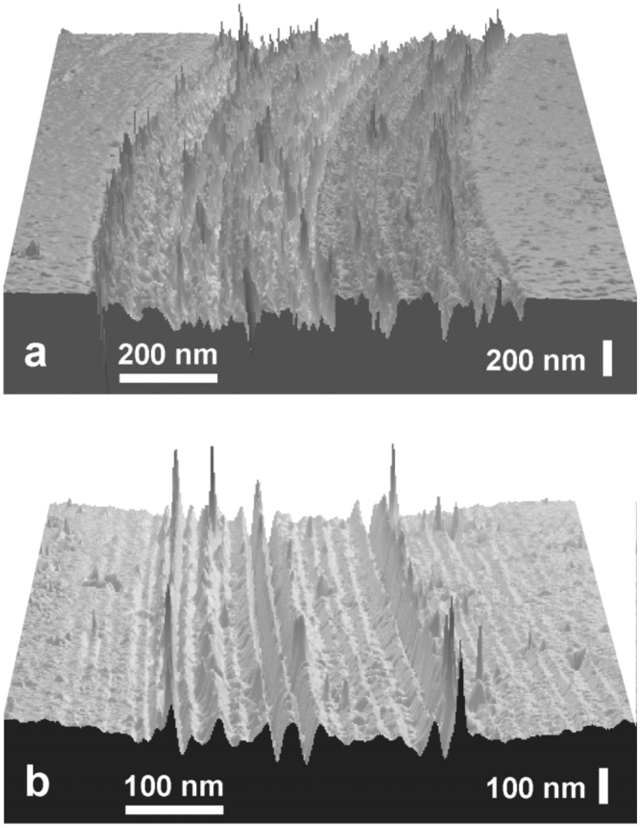

Fig. 7. Optical profilometry micrographs of the disc wear tracks after 90 m sliding of on-axis TiN coatings against (a) an uncoated 100Cr6 ball and (b) an alumina ball (test parameters: friction force: 10 N, sliding speed: 0.1 m s^{-1}, temperature: 25 °C, relative humidity: 60%).

due to the two different deposition arrangements. Comparing the wear behaviour of all disc/ball couples investigated, the TiN/Al_2O_3 couple provides the best wear performance after 90 m of sliding. The highest wear rates were found for the TiN/100Cr6 couple in this short distance test due to the high adhesion between the steel and the TiN surfaces [1] and the transfer layer formation. Long test durations (1000 m) drop the wear down to very low rates because of pure sliding on the transfer layer, resulting in higher pin wear rates.

4. Conclusions

Nearly stoichiometric titanium nitride (TiN) coatings with very smooth surfaces and excellent adhesion were successfully deposited onto steel substrates (high speed steels and corrosion resistant steels) at room temperature with a multi-spot PLD system. The steel substrates were mounted parallel (on-axis technique) and normal (off-axis) to the target surface leading to completely different deposition conditions. In the case of the off-axis grown films the ablated particles can only hit the substrate surface after scattering with other atoms in the vacuum chamber. The scattering reduces both the energy and the flux of the deposited species (atoms, ions, clusters) at the growing film surface. Thus, growth rates, micro-columnare structures, fibre textures and mechanical properties of the TiN films are strongly dependent on the deposition arrangement. The higher the energy of the deposited species, the higher are the compressive residual stresses and, thus, the hardnesses and elastic moduli. In contrast, the chemical composition was not influenced by the different deposition conditions. Compared to other PVD or CVD coatings deposited at elevated temperatures, very low wear coefficient have been observed for the disc/pin couples (TiN/100Cr6, TiN/Al_2O_3) investigated in the pin-on-disc test.

Acknowledgments

Financial support of this work by the Austrian Federal Ministry of Traffic, Innovation and Technology, the Austrian Industrial Research Promotion Fund (FFF), the Government of Styria, the Technologie Impulse Gesellschaft mbH in the frame of the Kplus Programme and the European Union is highly acknowledged.

References

[1] K. Holmberg, A. Matthews, Coatings Tribology, Elsevier, Amsterdam, 1994.
[2] D.B. Chrisey, G.K. Hubler, Pulsed Laser Deposition of Thin Films, Wiley, New York, 1994.
[3] H.D. Gu, K.M. Leung, Surf. Coat. Technol. 110 (1998) 153.
[4] V. Craciun, D. Craciun, Appl. Surf. Sci. 138–139 (1999) 593.
[5] A.R. Phani, J.E. Krzanowski, Appl. Surf. Sci. 174 (2001) 132.
[6] R. Chowdhury, R.D. Vispute, J. Mater. Res. 11 (1996) 1458.
[7] O. Auciello, T. Barnes, Thin Solid Films 181 (1989) 65.
[8] N. Biunno, J. Narayan, Appl. Phys. Lett. 54 (1989) 1519.
[9] R. Ebner, W. Waldhauser, W. Lenz, Proc. Materials Week 2001, Munich, 2001.
[10] J.A. Thornton, J. Vac. Sci. Technol. 11 (1974) 666.
[11] J.E. Greene, in: D.T.J. Hurle (Ed.), Handbook of Crystal Growth, vol. 1, Elsevier, Amsterdam, 1993, p. 640.
[12] W. Ensinger, Nucl. Instrum. Meth. Phys. Res. B 127–128 (1997) 796.
[13] T.C. Chou, J. Appl. Phys. 67 (1990) 2670.
[14] J. Pelleg, L.Z. Zevin, S. Lungo, Thin Solid Films 197 (1991) 117.
[15] I. Petrov, L. Hultman, U. Helmersson, J.-E. Sundgren, J.E. Greene, Thin Solid Films 169 (1989) 299.
[16] D.S. Williams, F.A. Baiocchi, R.C. Beairsto, J. Vac. Sci. Technol. B 5 (1987) 1723.
[17] H. Windischmann, J. Appl. Phys. 62 (1987) 1800.
[18] Y.M. Chen, G.P. Yu, J.-H. Huang, Surf. Coat. Technol. 141 (2001) 156.
[19] J.-H. Huang, Y.-P. Tsai, G.-P. Yu, Thin Solid Films 355–356 (1999) 440.
[20] L. Alberts, R. Leutenecker, G.K. Wolf, Surf. Coat. Technol. 84 (1996) 443.
[21] P. Huber, D. Manova, S. Mändl, B. Rauschenbach, Surf. Coat. Technol. 156 (2002) 176.
[22] B. Major, R. Ebner, Appl. Phys. A 69 (1999) 921.

[23] D.S. Rickerby, G. Eckold, K.T. Scott, I.M. Buckley-Golder, Thin Solid Films 154 (1987) 125.
[24] V. Sedlácek, Metallic Surfaces, Films and Coatings, Elsevier, Amsterdam, 1992.
[25] H. Jehn, G. Reiners, N. Siegel, DIN-Fachbericht 39, Beuth-Verlag, Berlin, 1993.
[26] J.M. Lackner, W. Waldhauser, W. Lenz, R. Ebner, B. Major, T. Schöberl, Prakt. Metallogr. Sonderband 34 (2003) 291.